Automated determination of cardiac rest period on whole-heart coronary magnetic resonance angiography by extracting high-speed motion of coronary arteries

Hiroya Asou[a,b,*], Naoyuki Imada[a], Yuichi Nishiyama[c], Tomoyasu Sato[a], Katsuhiro Ichikawa[d]

[a] Department of Radiology, Tsuchiya General Hospital, 3-30 Nakajima-cho, Hiroshima-shi, Hiroshima 730-8655, Japan
[b] Graduate School of Medical Science, Kanazawa University, 5-11-80 Odachino, Kanazawa-shi, Ishikawa 920-0942, Japan
[c] Department of Biomedical Science and Technology, Graduate School of Biomedical Sciences, Tokushima University, 3-18-15 Kuramoto-cho, Tokushima-shi, Tokushima 770-8503, Japan
[d] Institute of Medical, Pharmaceutical and Health Sciences, Kanazawa University, 5-11-80 Odachino, Kanazawa-shi, Ishikawa 920-0942, Japan

A R T I C L E   I N F O

A B S T R A C T

Purpose: The aim of the present study was to develop an automated system for determining the cardiac rest period during whole-heart coronary magnetic resonance angiography (CMRA) examination.
Materials and methods: Ten healthy male volunteers (25–51 years old, 50–77 beats/min heart rate) were enrolled in this prospective study. A motion area map was generated from a cine image set by extracting high-speed component of cardiac motion, and it was used to specify the rest period in the proposed CMRA. In conventional CMRA, the rest period was determined based on the visual inspection of cine images. Agreement of the start time, end time, and trigger time between the two methods was assessed by the Bland-Altman plot analysis. Two observers visually evaluated the quality of the curved planar reformation (CPR) image of the coronary arteries.
Results: The proposed method significantly prolonged the start time (mean systematic difference 37.7 ms, $P < 0.05$) compared with the conventional method. Good agreement was observed for the end time (mean systematic difference 8.9 ms) and trigger time (mean systematic difference -28.8 ms) between the two methods. A significantly higher image quality ($P < 0.05$) was provided for the left circumflex artery in the proposed CMRA (mean grading score 3.88) than in conventional CMRA (mean grading score 3.68).
Conclusion: Our system enabled detection of the rest period automatically without operator intervention and demonstrated somewhat higher image quality compared with conventional CMRA. Its use may be useful to improve the imaging workflow for CMRA in clinical practice.

1. Introduction

Coronary artery disease (CAD) is one of the most common causes of death [1, 2]. There are several methods to diagnosis CAD such as X-ray coronary angiography [3] and coronary computed tomography (CT) angiography [4]. However, radiation exposure to patients and its risk of carcinogenesis are serious concerns, especially for children [5, 6]. Furthermore, these imaging techniques using contrast materials are inapplicable for patients with severe kidney dysfunction.

Along with advances in magnetic resonance imaging (MRI), whole-heart coronary magnetic resonance angiography (CMRA) enables non-invasive, radiation-free, and contrast material-free examination of CAD [7, 8]. Suppression of motion artifacts is particularly important for CMRA. Data acquisition should be carried out during the mid- to late-

diastolic phase of the heart (cardiac rest period) in combination with the end-expiration phase. Diaphragm navigators and electrocardiogram (ECG)-gate navigators are often used in conventional CMRA. Although the diaphragm navigator automatically detects the end-expiration phase, operators are required to manually specify the cardiac rest period by visual inspection of cardiac motion on cine images. Therefore, image quality is highly dependent on the operator's skill.

Accordingly, the aim of the present study was to develop an automated system to determine the cardiac rest period during CMRA. By analyzing the high-speed motion of the heart in a cine image set, we specified the cardiac phase optimal for data acquisition. The proposed CMRA produced higher quality coronary artery images than conventional CMRA.

---

* Corresponding author at: Department of Radiology, Shimane University Hospital, 89-1 Enya-cho, Izumo-shi, Shimane 693-8501, Japan.
E-mail address: hasou@med.shimane-u.ac.jp (H. Asou).

2. Methods

2.1. Subjects

The subjects consisted of ten healthy male volunteers without heart or respiratory diseases. The mean age and mean heart rate were 36.5 years old (range 25–51) and 65.1 beats/min (range 50–77), respectively. Ethical approval for this prospective study was obtained from the Ethical Committee of Tsuchiya General Hospital. Informed consent was obtained from each subject.

2.2. MRI scanner and image sequences

A 1.5-tesla MRI scanner (Intera Achieva, Philips Healthcare, Best, Netherlands) with a 5-channel SENSitivity Encoding (SENSE) cardiac phased array coil was used in all imaging procedures. A weight was placed on the abdomen, and an abdominal compression belt was rolled tightly along the side of the ribs to reduce abdominal movement [9].

Cardiac cine imaging was conducted using ECG-gated two-dimensional (2-D) true fast imaging with steady state precession (true FISP) sequence under breath holding. The imaging parameters were as follows: 3.3 ms repetition time (TR), 1.65 ms echo time (TE), 60 degree flip angle, 400 × 400 mm field of view (FOV), 176 × 133 matrix, and 6 mm slice thickness. Four-chamber long-axis planes (80 frames per heart cycle) were scanned to evaluate myocardial wall motion.

The proposed and conventional CMRA were carried out using a 3-dimensional (3-D) segmented true FISP sequence under free breathing. The imaging parameters were as follows: 4.14 ms TR, 2.07 ms TE, 80 degree flip angle, 300 × 300 mm FOV, 224 × 224 matrix, and 0.85 mm slice thickness. The diaphragm navigator was located on the top of the right diaphragm, and scan data were collected in the end-expiratory phase. For conventional CMRA, operators manually determined the data acquisition timing (cardiac rest period) based on visual inspection of the cine images. Three radiological technologists with > 5 years of experience in CMRA imaging assessed the cardiac phase representing the least motion of the heart, and determined the start time and end time by mutual agreement.

2.3. High-speed cine image

The proposed CMRA was conducted immediately after conventional CMRA. In the proposed CMRA, a cine image set was analyzed to specify cardiac regions representing high-speed motion (Fig. 1). A one-dimensional (1-D) temporal profile of the pixel value was extracted from a cine image set, and cardiac motion $F(k)$ was generated by Fourier transformation of the profile as follows:

$$F(k)_{(x,y)} = \sum_{n=0}^{N-1} f(n)_{(x,y)} e^{-j2\pi kn/N} \tag{1}$$

where k is the frequency (Hz), $f(n)_{(x, y)}$ is the 1-D temporal profile at an arbitrary coordinate on the 2-D cine image, n is the frame number of the cine image, N is the total frame number, and j is the imaginary number. Moreover, the high-speed component of the cardiac motion $X(k)$ was extracted using a high-pass filter, and a preliminary high-speed cine image $F'(n)$ was obtained by inverse Fourier transformation of $X(k)$ as follows:

$$X(k)_{(x,y)} = F(k)_{(x,y)} \times H(k)_{(x, y)} \tag{2}$$

$$F'(n)_{(x,y)} = \frac{1}{N} \sum_{n=0}^{N-1} X(k)_{(x,y)} e^{j2\pi kn/N} \tag{3}$$

where $H(k)$ is a filter coefficient. The filter coefficient was calculated in the preliminary study. When $H(k)$ was set at 83%, the high-speed component was successfully differentiated from the low-speed component.
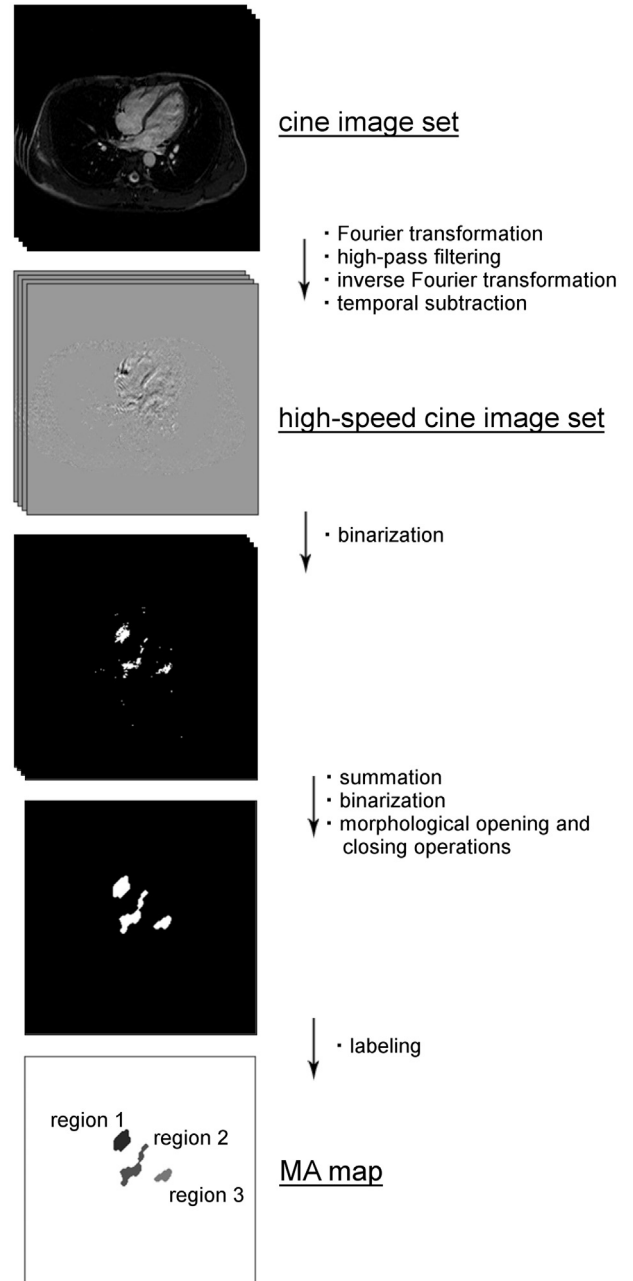

Fig. 1. Image processing during the proposed whole-heart coronary magnetic resonance angiography (CMRA). The high-speed component of cardiac motion was extracted from a cine image set by combination of Fourier transformation, high-pass filtering, inverse Fourier transformation, and temporal subtraction processing, resulting in a high-speed cine image set. A motion area (MA) map was then created by the threshold and binarization processing of the high-speed cine image set. The MA map shows three labeled regions representing high-speed cardiac motion.

After the inverse Fourier transformation, temporal subtraction processing [10] was conducted to emphasize the high-speed cardiac motion as follows:

$$P(i)_{(x,y)} = F'(n+1)_{(x,y)} - F'(n)_{(x,y)} \tag{4}$$

where i is the frame number of the subtraction image set. The subtraction image $P(i)$ was defined as a high-speed cine image and used for creating the motion area (MA) map.
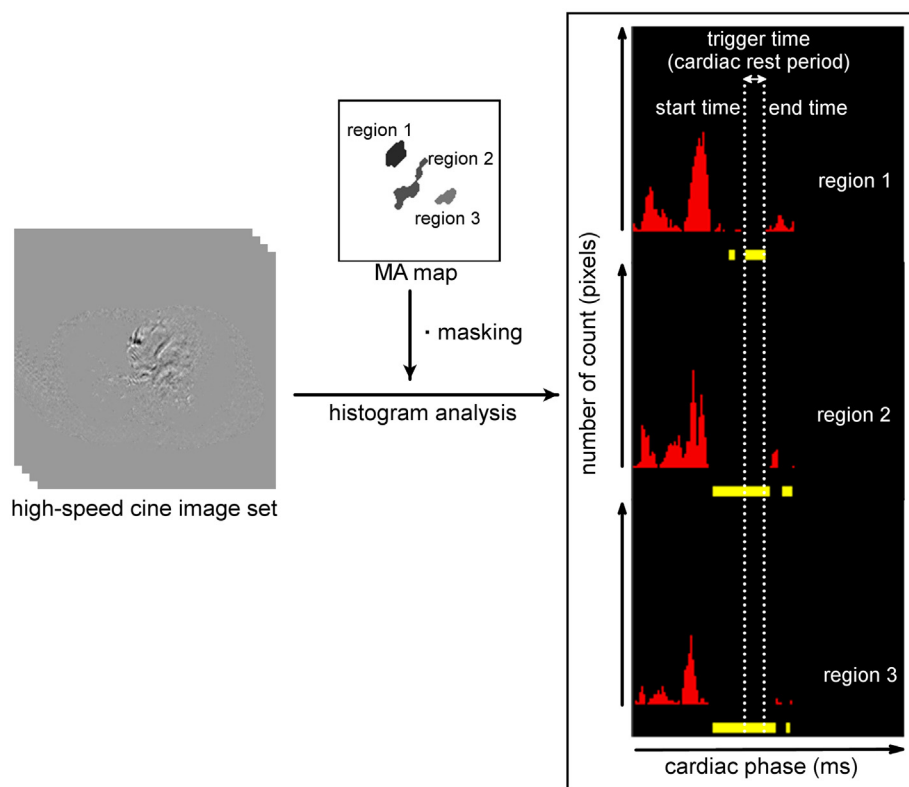
Fig. 2. Determination of the cardiac rest period using a motion area (MA) map. Start time, end time, and trigger time were optimized using the MA map. High-speed cine images were masked with the MA map, and the number of pixels within each labeled region was counted based on the cardiac phase. Yellow colored bars below each histogram indicate cardiac phase with counting zero pixels. The time period with zero pixels simultaneously in three regions was defined as the rest period. (For interpretation of the references to color in this figure legend, the reader is referred to the web version of this article.)

2.4. Motion area map

Each high-speed cine image was converted to a binary image by threshold processing. The threshold level was set to −10% of a spectral peak. The binary images were summed, followed by the binarization process again. Noise signals were then removed by morphological opening and closing operations [11], and three regions representing high-speed cardiac motion were specified. Subsequently, these regions were labeled with 1, 2, and 3, and the labeled image was defined as a MA map. Regions 1 and 3 show displacement areas of the right coronary artery (RCA) and left anterior descending artery (LAD), respectively. Region 2 was produced by high-speed signal components, including the blood flow into the left atrium and the cardiac septal motion (Supplementary Video).

Data acquisition timing for the proposed CMRA was determined using the MA map. The number of pixels within the labeled regions was counted in each frame of the high-speed cine image set, and a cumulative histogram was created based on the cardiac phase. Start time, end time, and trigger time were determined based on the duration of the cardiac phase in which the pixel counts were simultaneously zero in the three regions (Fig. 2). We developed a computer program for image processing and MA map analysis (Fig. 3).

2.5. Visual evaluation of image quality

Curved planar reformation (CPR) images of RCA, LAD, and the left circumflex artery (LCX) were created on a 3-D workstation (AZE Virtual Place, AZE Co., Ltd., Tokyo, Japan). Two observers, a radiologist with 5 years of experience in CMRA diagnosis, and a radiological technologist with 5 years of experience in CMRA imaging, examined the CPR image quality. They visually evaluated the sharpness of vessel edges using five grades (scored from 1 to 5 points: 1 for strongly blurred edges, 2 for moderately blurred edges, 3 for mildly blurred edges, 4 for slightly blurred edges, and 5 for no blurred edges).

2.6. Statistical analysis

Differences in the mean grading score were evaluated by the Wilcoxon signed rank test. Agreement of the start time, end time, and trigger time between the two methods was assessed by the Bland-Altman plot analysis [12]. Differences in start time, end time, and trigger time were analyzed by the paired-t-test. $P < 0.05$ was considered significant in all statistical analyses.

3. Results

3.1. Bland-Altman plot analysis

Bland-Altman plot analysis demonstrated high agreement for end time and trigger time between conventional CMRA and the proposed CMRA. The mean systematic differences in end time and trigger time were 8.9 ms and −28.8 ms, respectively (95% confidence interval (CI), −14.9 to 32.7 ms for end time and −73.1 to 15.5 ms for trigger time). Moreover, there was a low agreement for start time between the two methods. The mean systematic difference was 37.7 ms for start time, with a 95% CI of 14.0 to 61.4 ms (Fig. 4).

3.2. Comparison of start time, end time, and trigger time between the two methods

As shown in Table 1, the mean start time in the proposed CMRA was significantly longer than that in conventional CMRA ($P = 0.003$). Although the mean end time with the proposed method was longer than that with the conventional method, there were no significant differences ($P = 0.210$). The mean trigger time with the proposed method was shorter than that with the conventional method, but the difference was not significant ($P = 0.088$).
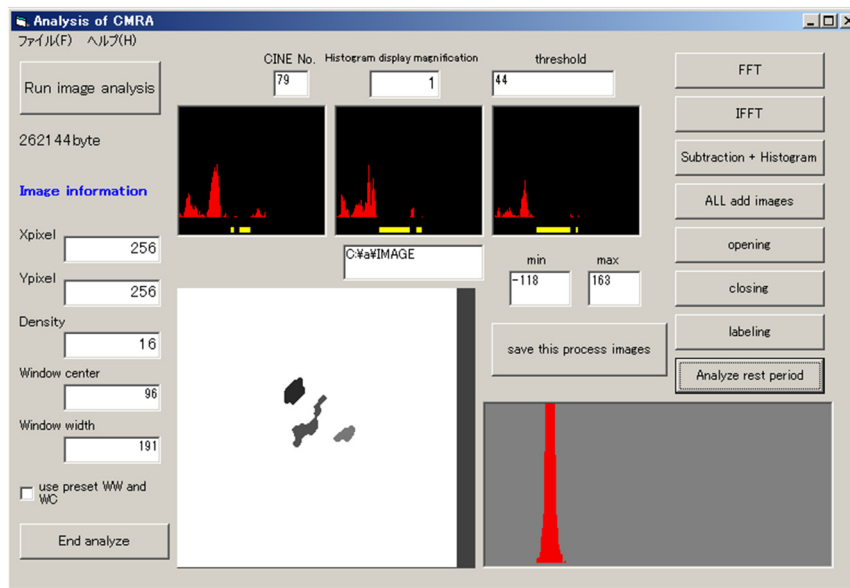
Fig. 3. Screen shot of the developed program showing an analysis of the cardiac rest period.
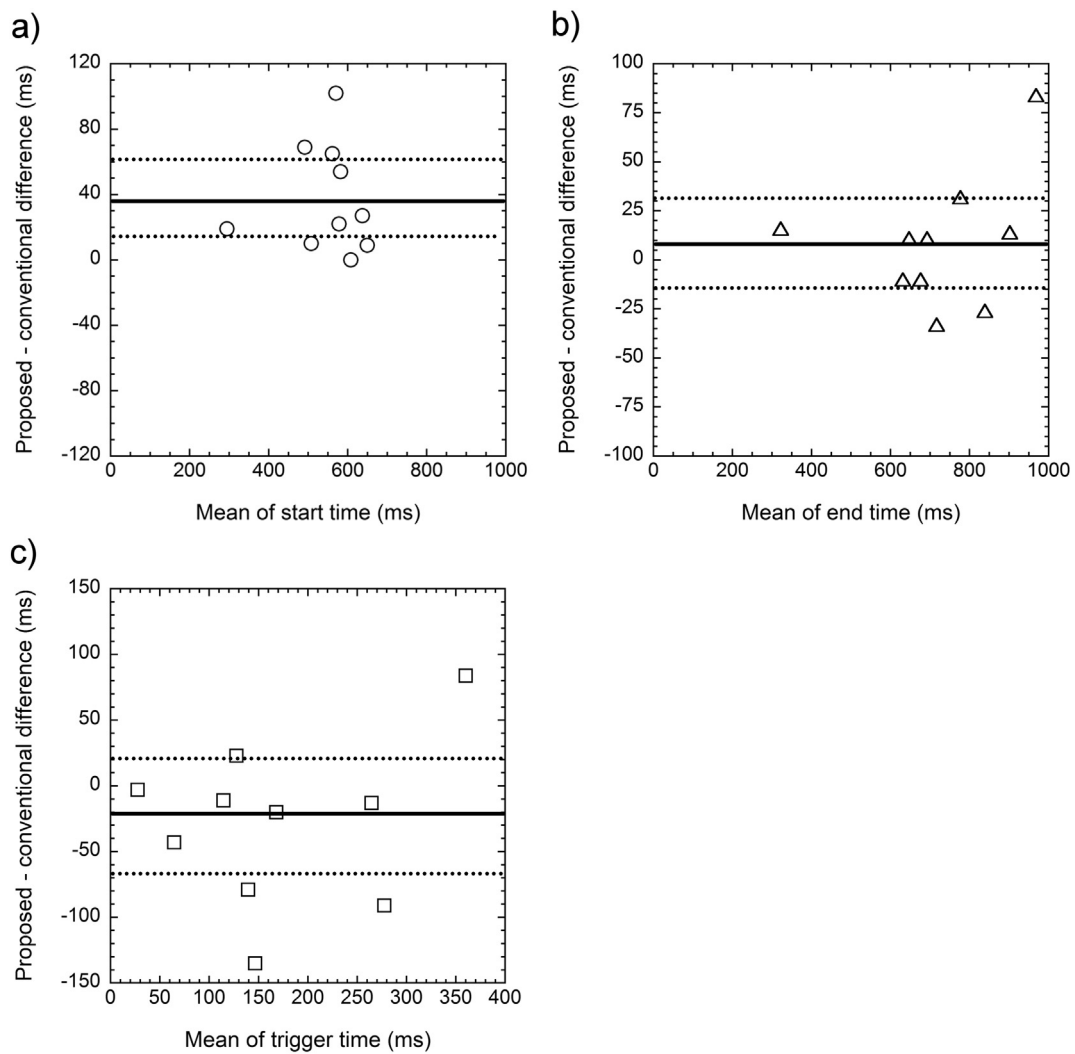

Fig. 4. Bland-Altman plot analysis demonstrated a good agreement for end time (b) and trigger time (c) between the two whole-heart coronary magnetic resonance angiography methods. There was a low agreement for start time (a) between the two methods. The central horizontal line indicates the mean systematic difference. Upper and lower dotted lines represent 95% confidence intervals.

Table 1
Comparison of start time, end time, and trigger time between the two whole-heart coronary magnetic resonance angiography methods.

	Conventional	Proposed	*P*-value
Start time (ms)	529 ± 103	567 ± 103	0.003
End time (ms)	713 ± 174	722 ± 184	0.210
Trigger time (ms)	183 ± 99	155 ± 114	0.088

Data are presented as the mean ± standard deviation.

3.3. Visual evaluation of CPR image quality

Fig. 5 shows a typical example of a CPR image of coronary arteries, and Table 2 summarizes the grading scores for CPR image quality. Although the proposed CMRA provided slightly higher grading scores for RCA ($P = 0.35$) and LAD ($P = 0.15$) compared with conventional CMRA, there were no significant differences. However, the proposed method provided a significantly higher grading score for the LCX ($P = 0.02$) compared with the conventional method.
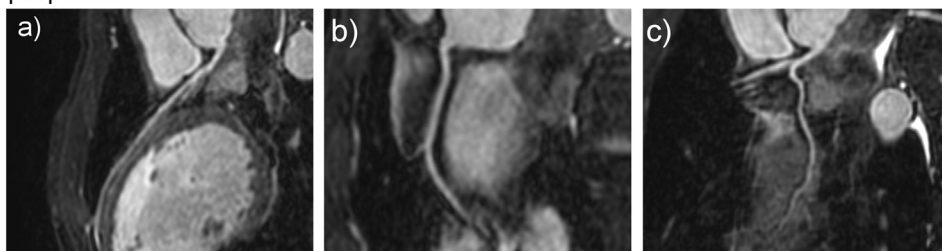
4. Discussion

In the present study, we developed an effective method to determine the cardiac rest period for whole-heart CMRA. We focused on cardiac regions representing high-speed motion and successfully extracted a cardiac phase suitable for data acquisition. This resulted in almost the same trigger time and end time between the proposed and conventional methods. The proposed method improved the quality of CPR images of the coronary arteries.
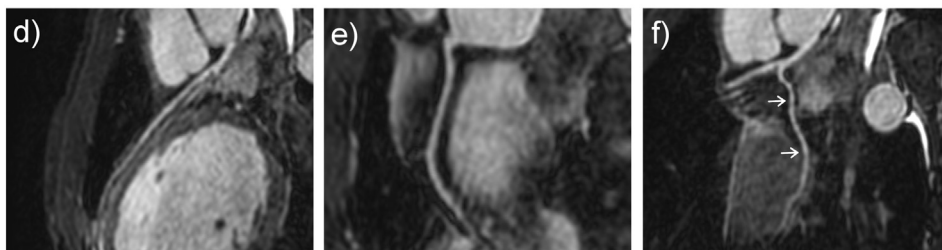
Several attempts have been made to extract the rest period during CMRA. Ustun et al. developed the FREEZE algorithm, which detects an optimal cardiac phase for data acquisition by analyzing myocardial displacement, resulting in improved vessel sharpness on images [13]. Jahnke et al. demonstrated automated detection of the rest period by cross-correlation analysis of the coronary position between consecutive cine images [14]. However, with these semi-automated techniques, image quality may be somewhat affected by the position of the operator-defined ROI. In contrast, our proposed method is a fully automated technique. It enables complete removal of user intervention and reduces complicated procedures for determining the rest period, leading to reproducible results for physicians.

In conventional CMRA, operators need to have sufficient experience

Table 2
Comparison of the grading score for curved planar reformation image quality between the two whole-heart coronary magnetic resonance angiography methods.

	Conventional	Proposed	*P*-value
RCA	4.13 ± 0.27	4.18 ± 0.29	0.35
LAD	4.03 ± 0.25	4.10 ± 0.32	0.15
LCX	3.68 ± 0.39	3.88 ± 0.46	0.02

RCA right coronary artery, *LAD* left anterior descending artery, *LCX* left circumflex artery.
Data are presented as the mean ± standard deviation.

and be highly skilled to determine the rest period because each coronary artery exhibits the least motion in different cardiac phases. Sato et al. recently reported a fully automated method to determine the rest period based on a template-matching technique [15]. They estimated consecutive displacement of the position of the RCA by comparing a template image with cine images. However, this method focused only on the motion of the RCA. The prime benefit of our technique is that data acquisition is carried out during the cardiac phase in which both the RCA and LCA show the least motion at the same time. As a result, the proposed CMRA demonstrated a clear advantage with respect to the CPR image quality. This may be attributed to our unique approach for analyzing the motion of coronary arteries. Our proposed method is expected to increase diagnostic accuracy by improving CPR image quality.

The Bland-Altman plot analysis revealed good agreement for the end time and trigger time between the two methods, suggesting practical applicability to clinical CMRA. However, the proposed method prolonged the start time compared with the conventional method, resulting in a slight reduction in the trigger time. The difference in trigger time was approximately 40 ms between the two methods, and similar results were reported in several studies using other techniques for automatic estimation of the rest period [13, 15]. The coronary artery moves slowly at the start of the rest period, but moves rapidly at the end [15]. In conventional CMRA, operators possibly treated the slow movement as being stopped. In contrast, the proposed method allowed to track the slow movement (see Supplementary Video), which may contribute to the prolongation of the start time. Although the short trigger time increases the total examination time, it is generally advantageous for reducing potential motion artifacts [16, 17]. These

proposed

conventional

Fig. 5. Curved planar reformation (CPR) image of left anterior descending artery (LAD) (a and c), right coronary artery (RCA) (b and e), and left circumflex artery (LCX) (c and f) of a 36-year-old man. The proposed whole-heart coronary magnetic resonance angiography (CMRA) improved the sharpness of the edge of the LCX compared with conventional CMRA (*white arrows*). RCA and LAD had a similar sharpness with the two methods.

findings may be associated with the improved CPR image quality of the LCX. Use of the proposed method slightly changed the trigger time; therefore, its influence seems to be negligible in terms of the total examination time.

The limitation of the present study is that the performance of the proposed method was assessed in a small population comprising healthy male volunteers. The heart rate is generally higher in female than in male [18, 19], and it may be an important factor influencing image quality in CMRA. Leiner et al. reported effective suppression of motion artifacts by correcting heart rate variability and demonstrated an improved image quality in CMRA [20]. In coronary CTA, Hoffmann et al. reported a negative correlation between image quality and heart rate, and noted degeneration in image quality at a heart rate of over 80 beats/min [21]. It is unclear whether the proposed method successfully works in patients with fast heart rates. Another limitation is that the CPR image quality was not evaluated quantitatively. Contrast-enhanced CMRA achieves a good signal uniformity in the coronary lumen, and the inverse of the average transition width of the coronary lumen profile is often calculated as the quantitative value representing the sharpness of the vessels [22, 23]. For the present study, we could not quantitate the vessel sharpness in the same way due to the non-uniform signal intensity in the lumen. Further studies are required to clarify the clinical effectiveness of our system.

5. Conclusions

In this study, we developed a fully automated system to specify the cardiac rest period during whole-heart CMRA. Our system enabled determination of the optimal cardiac phase for data acquisition and improved quality of coronary CPR images in the preliminary study including 10 healthy male volunteers. Its use may promote efficiency in the imaging operation by removing operator intervention.

Supplementary data to this article can be found online at https://doi.org/10.1016/j.clinimag.2018.07.006.

Conflicts of interest

The authors declare that they have no conflicts of interest.

References

[1] Okrainec K, Banerjee DK, Eisenberg MJ. Coronary artery disease in the developing world. Am Heart J 2004;148:7–15.

[2] Deaton C, Froelicher ES, Wu LH, Ho C, Shishani K, Jaarsma T. The global burden of cardiovascular disease. Eur J Cardiovasc Nurs 2011;10:S5–13.

[3] Mollet NR, Cademartiri F, Van Mieghem CAG, Runza G, McFadden EP, Baks T, Serruys PW, Krestin GP, De Feyter PJ. High-resolution spiral computed tomography coronary angiography in patients referred for diagnostic conventional coronary angiography. Circulation 2005;112:2318–23.

[4] Nieman K, Oudkerk M, Rensing BJ, van Ooijen P, Munne A, van Geuns RJ, de Feyter PJ. Coronary angiography with multi-slice computed tomography. Lancet 2001;357:599–603.

[5] Pearce MS, Salotti JA, Little MP, McHugh K, Lee C, Kim KP, Howe NL, Ronckers CM, Rajaraman P, Sir Craft AW, Parker L, Berrington de Gonzalez A. Radiation exposure from CT scans in childhood and subsequent risk of leukaemia and brain tumours: a retrospective cohort study. Lancet 2012;380:499–505.

[6] Brenner DJ, Elliston CD, Hall EJ, Berdon WE. Estimated risks of radiation-induced fatal cancer from pediatric CT. Am J Roentgenol 2001;176:289–96.

[7] Kim WY, Danias PG, Stuber M, Flamm SD, Plein S, Nagel E, Langerak SE, Weber OM, Pedersen EM, Schmidt M, Botnar RM, Manning WJ. Coronary magnetic resonance angiography for the detection of coronary stenoses. N Engl J Med 2001;345:1863–9.

[8] Weber OM, Martin AJ, Higgins CB. Whole-heart steady-state free precession coronary artery magnetic resonance angiography. Magn Reson Med 2003;50:1223–8.

[9] Morita S, Suzuki K, Machida H, Fujimura M, Ohnishi T, Imura C, Ueno E. Compression belt for navigator-triggered trueFISP whole-heart coronary magnetic resonance angiography: study in healthy volunteers. Magn Reson Med Sci 2008;7:79–83.

[10] Doi K. Computer-aided diagnosis in medical imaging: historical review, current status and future potential. Comput Med Imaging Graph 2007;31:198–211.

[11] Yu-Qian Z, Wei-Hua G, Zhen-Cheng C, Jing-Tian T, Ling-Yun L. Medical images edge detection based on mathematical morphology. Conf. Proc. Int. Conf. IEEE Eng. Med. Biol. Soc. vol. 6. 2005. p. 6492–5.

[12] Bland JM, Altman DG. Statistical methods for assessing agreement between two methods of clinical measurement. Lancet 1986;327:307–10.

[13] Ustun A, Desai M, Abd-Elmoniem KZ, Schar M, Stuber M. Automated identification of minimal myocardial motion for improved image quality on MR angiography at 3 T. AJR Am J Roentgenol 2007;188:W283–90.

[14] Jahnke C, Paetsch I, Nehrke K, Schnackenburg B, Bornstedt A, Gebker R, Fleck E, Nagel E. A new approach for rapid assessment of the cardiac rest period for coronary MRA. J Cardiovasc Magn Reson 2005;7:395–9.

[15] Sato T, Okada T, Kuhara S, Togashi K, Kanaya S, Minato K. Automatic identification of the cardiac rest period using template updating for magnetic resonance coronary angiography. Adv Biomed Eng 2016;5:26–31.

[16] Ferreira PF, Gatehouse PD, Mohiaddin RH, Firmin DN. Cardiovascular magnetic resonance artefacts. J Cardiovasc Magn Reson 2013;15:41.

[17] Sakuma H, Ichikawa Y, Suzawa N, Hirano T, Makino K, Koyama N, Van Cauteren M, Takeda K. Assessment of coronary arteries with total study time of less than 30 minutes by using whole-heart coronary MR angiography. Radiology 2005;237:316–21.

[18] Sagie A, Larson MG, Goldberg RJ, Bengtson JR, Levy D. An improved method for adjusting the QT interval for heart rate (the Framingham Heart Study). Am J Cardiol 1992;70:797–801.

[19] Singh JP, Larson MG, O'Donnell CJ, Tsuji H, Evans JC, Levy D. Heritability of heart rate variability: the Framingham Heart Study. Circulation 1999;99:2251–4.

[20] Leiner T, Katsimaglis G, Yeh EN, Kissinger KV, Van Yperen G, Eggers H, Manning WJ, Botnar RM. Correction for heart rate variability improves coronary magnetic resonance angiography. J Magn Reson Imaging 2005;22:577–82.

[21] Hoffmann MHK, Shi H, Manzke R, Schmid FT, De Vries L, Grass M, Brambs H-J, Aschoff AJ. Noninvasive coronary angiography with 16-detector row CT: effect of heart rate. Radiology 2005;234:86–97.

[22] Deshpande VS, Wielopolski PA, Shea SM, Carr J, Zheng J, Li D. Coronary artery imaging using contrast-enhanced 3D segmented EPI. J Magn Reson Imaging 2001;13:676–81.

[23] Addy NO, Ingle RR, Wu HH, Hu BS, Nishimura DG. High-resolution variable-density 3D cones coronary MRA. Magn Reson Med 2015;74:614–21.